This paper is to be presented at the
IAMG Annual Meeting
Cancùn, Mexico
September 6-12, 2001

Fluvial meandering channelized reservoirs: a stochastic & process-based approach

S. Lopez[1,2], A. Galli[1] & I. Cojan[2]

1: Centre de Géostatistique,
Ecole des Mines de Paris
35, rue Saint Honoré
77305 Fontainebleau
France

2: Laboratoire de Sédimentologie, C.G.E.S.,
Ecole des Mines de Paris
35, rue Saint Honoré
77305 Fontainebleau
France

Abstract

This paper presents a stochastic and process-based approach to the modeling of meandering channelized reservoirs which provides accurate and realistic 3D representations of the simulated sand bodies. It focuses on such modeling at the reservoir scale trying to address a new type of models combining ideas from process based models and stochastic models. The first part deals with equations driving channel motion and the modeling of channel centerline evolution. Then fluvial deposits along this centerline are modeled. Finally in a last part a few stochastic parameters are studied in order to address their influence on vertical proportion curves of facies.

1 Introduction

These last 15 years considerable work has been undertaken to establish and implement stochastic models for reservoir characterization. Most, if not all, of the stochastic models currently available (pixel or object oriented) are phenomenological: they aim at reproducing at the reservoir scale the results of the sedimentation and not the underlying processes. Concurrently, deterministic process based models have been developed. These models generally consider the basin scale and are usually unsuitable for reservoir modeling because of the need for many parameters. Moreover these parameters are generally difficult to assess and varying with time. In this paper we aim at addressing a new type of models

combining ideas from process based models and stochastic models in a simple way for the modeling of meandering channelized reservoirs at the scale of the oil reservoir.

2 Governing equations

Natural rivers meander because of the helical pattern of their flow velocity field. The secondary flow which is normal to the channel centerline pushes the main flow alternatively against one bank and then the other. The bank against which the velocity is the highest is eroded while deposition occurs at the opposite bank. This combination of erosion and deposition accounts for meander development and progressive channel migration. As a result, to quantify this migration the flow velocity field inside the channel has to be estimated.

2.1 Computation of the flow velocity field

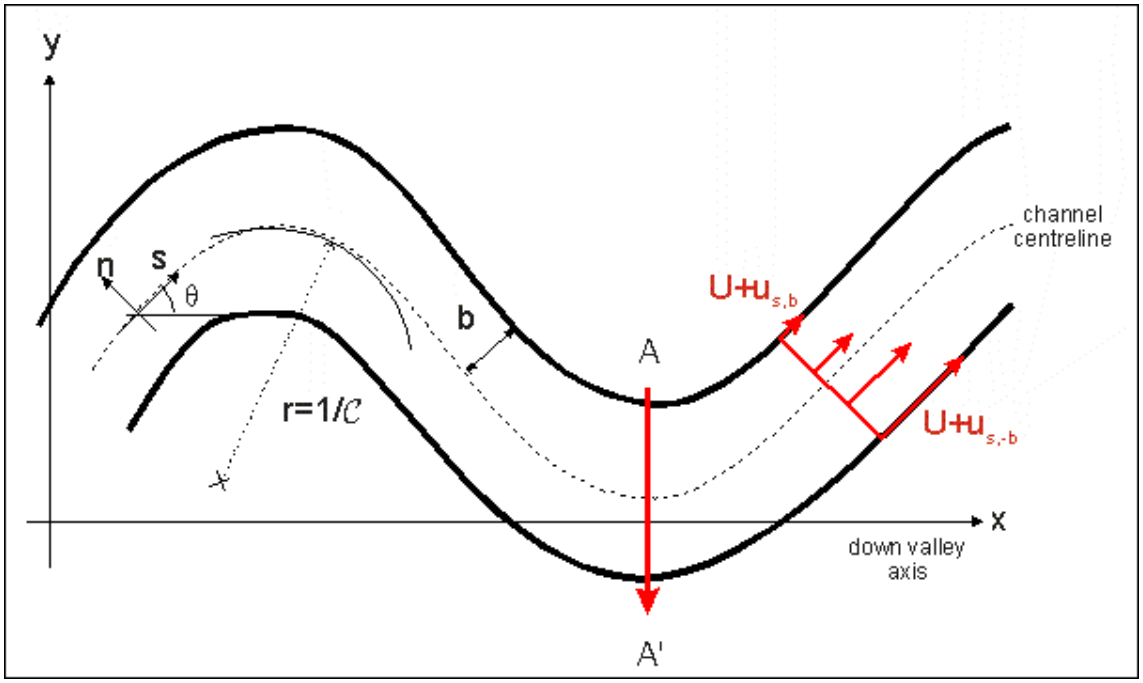

Figure 1: Planar sketch summarizing the main notations. The river migrates from A to A'. (cf. text for other notations)

In their pioneering work, Ikeda *et al.* [Ikeda et al., 1981] proposed a linearization of the Saint Venant equations for shallow water flows. They resorted to a curvilinear coordinate system (cf. 1) in which the velocity was expressed as the sum of the reach averaged velocity

of the flow, U and a local perturbation $u_{s,n}$ which was assumed to be small compared to U. In addition, the width of the river ($2b$), was taken to be constant, the maximum of the curvature of the channel centerline $\mathcal{C}$ was assumed to be small compared to b and finally, the flow was considered to be steady. Thus, Ikeda *ϵt al.* proposed an equation linking the flow velocity field inside the channel with its geometry and which had the following form :

$$\alpha \frac{\partial u_{s,b}}{\partial s} + \beta u_{s,b} = \chi \frac{\partial \mathcal{C}_s}{\partial s} + \delta \mathcal{C}_s \tag{1}$$

The left side of equation 1 concerns the flow velocity field with $u_{s,b}$ being the velocity local perturbation along the bank. The right side of equation 1 concerns the geometry of the channel with the channel centerline curvature $\mathcal{C}_s$. Physical and geometrical parameters such as the channel width and depth, the floodplain slope, the flow and some physical constant are included in the parameters α, β, χ and δ.

Many improvements of the work of the first work of Ikeda *ϵt al.* have been made since 1981, particularly concerning the convective transport of the main flow by the secondary flow ([Johanesson and Parker, 1989], [Sun, 1998]). Yet most of these improvements can be included in an equation with the same form as equation 1.

Direct implementation of the analytical solution of 1 involves a convolution product with an exponential kernel which leads to quick divergence. Consequently, the easiest way to proceed is to resort to classical finite differences, that once inserted into 1 provide a recurrence relation to compute the local perturbation of the flow velocity along the banks of a given channel [Sun et al., 1996].

Once the flow velocity field inside the channel is known, a bank retreat model is to be assumed to compute river migration.

2.2 Bank retreat model

Bank erosion rates and processes were relatively neglected research fields until recently and despite notable progress uncertainties remain to clearly take into account the complex and various processes leading to it [Thorne et al., 1997]. In order to have a general model Ikeda *ϵt al.* [Ikeda et al., 1981] proposed to model bank retreat in a simple way considering that it was only a function of the velocity of the flow against the bank. This implied that the floodplain they took into account was supposed to be constituted of a homogeneous material with spatially uniform properties. With these assumptions a simple Taylor development of the bank retreat ζ (expressed in $m.s^{-1}$ can be performed around U:

$$\begin{aligned} \zeta\left(U + u_{s,b}\right) &= \zeta\left(U\right) + \left.\frac{\partial \zeta}{\partial u}\right|_U u_{s,b} && (2) \\ &= \zeta\left(U\right) + E\left(U\right) u_{s,b} && (3) \end{aligned}$$

This development introduces the adimensional coefficient $E(U)$ which Ikeda *ϵt al.* called the erodibility coefficient and which is supposed to quantify the inclination of the

bank to be eroded. In the following $E(U)$ is simply noted E as the reach average velocity of the flow is supposed to be constant over time. This assumption can be seen as considering E as only representative of constant mechanical properties of the bank.

Finally, assuming that the mean river migration is null we have that the reach averaged velocity of the flow U is the limit between erosion and deposition leading to :

$$\zeta(U) = 0 \tag{4}$$

Which implies that we keep the simple bank retreat model :

$$\zeta_{s,b} = E u_{s,b} \tag{5}$$

2.3 Channel centerline evolution

With the set of the two equations 1 and 5 the migration of the channel centerline can be modeled. Many implementations have been proposed amongst which the ones by [Howard, 1992], [Howard, 1996] and [Sun et al., 1996].

As the bank retreat ζ has the dimension of a spatial velocity the time does not appear explicitly either in equation 1 or in equation 5. In the following, the assumption is that a migrating flood occurs each year (which is arbitrary) so that one iteration of the model represents a one year time lapse.

We applied the model to study the evolution of distinct initial channel centerlines, starting with nearly straight lines with uniformly distributed small perturbations (cf. figure 2). The first observation is the quick smoothing of the irregularities and the development of the same meandering period. This last result is well known in the geomorphologic community, the meandering wavelength being strongly correlated to the channel width. Yet though there is similarity in the pattern which are developing, the exact location of the loop is strongly influenced by the initial conditions.

Meanders do not evolve continuously and when both ends of a mature meander meet the river bypasses the loop. This process called neck cutoff will be here simply referred as cutoff. If avulsion processes are omitted the long term evolution of the river, will depend on those cutoff processes. As the cutoff location depends on the exact meander loop location it consequently depends on the initial centerline which influences the long term evolution of the meandering belt.

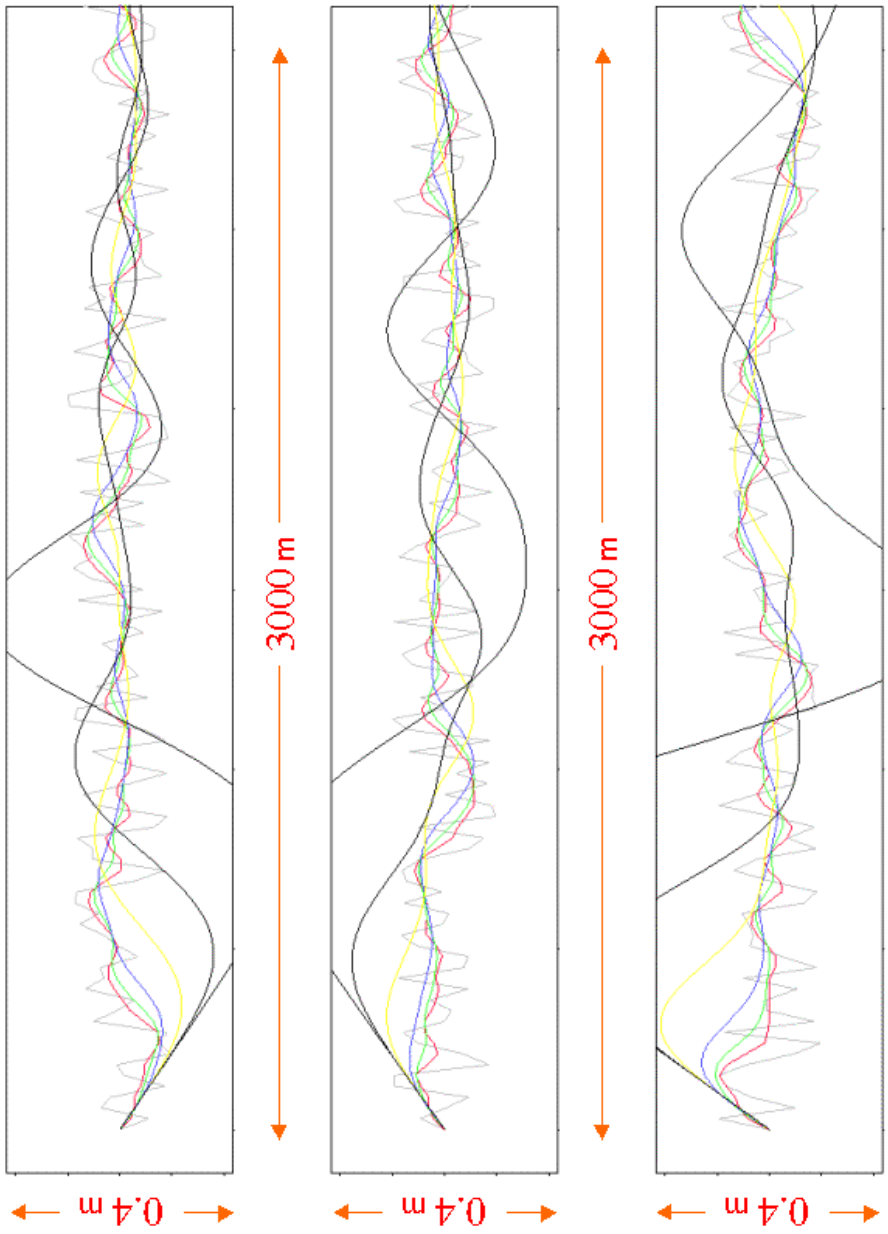

Figure 2: Study of the influence of the initial state of the channel centerline. The three initial conditions considered are nearly straight channel centerlines with uniformly distributed small perturbations. The color curves are the channel centerline locations after 50, 100 and 200 iterations. The two black lines correspond to the channel centerline location after 1000 iterations and 2000 iterations.

3 Modeling fluvial deposits

The first part dealt with the crude modeling of a curve evolution. In this part fluvial deposits are simulated to make this curve a more realistic river. To develop a fast efficient simulation we preferred to resort to heuristic approaches for deposition modeling, but still wanted to take account of the main processes governing fluvial deposition in a realistic way. For the present study, we left apart avulsions and crevasse splay processes and focused on three main types of deposits.

3.1 Simulated deposits

3.1.1 Overbank deposition

Overbank deposition occurs when the river floods. Water invades the land and deposits material whose grain-size and thickness decrease with the distance to the channel. This deposition accounts for the vertical development of the floodplain and is controlled by the frequency and intensity of successive floods.

To simulate these deposits, the channel convex hull is computed first. It is filled with a high proportion of sand and silt which can be seen as simulating a rough meandering belt. Then, outside the meandering belt, the exponential decreases of thickness and grain-size are controlled by two parameters. This approach is slightly different but inspired from the one by [Howard, 1996].

3.1.2 Point-bar deposits

When migrating, the channel leaves behind itself sandy deposits called point bar deposits which leads to lateral sand bar accretion. These meander loop deposits are the most common potential reservoir sands. Their three-dimensional architecture can be highly complex and variable ([Díaz-Molina et al., 1995]), with grain size usually decreasing with height. In the present model they are roughly simulated by filling the floodplain cells abandoned by the migrating channel with sand and fixing their thickness to the water elevation in the channel.

3.1.3 Oxbow-lake deposits

When the two ends of a meander belt meet, the river bypasses the mature meander belt, thus sealing the extremities of the abandoned part of the channel. This process is called neck cutoff and leads to the formation of an oxbow-lake where slow deposition of fine and cohesive sediment occurs. The resulting clay bodies form very cohesive and impermeable units often referred as mud-plugs between which oil is often trapped. The accurate simulation of mud-plugs is of high interest because they dramatically alter the connectivity of sand reservoirs. Herein, they are simulated by filling the abandoned channel with fine material and fixing its thickness to the previous channel depth.

3.2 Results

By storing the nature, age and thickness of deposits all over the floodplain we achieved very realistic 3D models of the floodplain. These 3D representations show the distribution of the sand bodies in possible reservoir units. The connections between them and the localization of mud plugs are easily identified too.

3.2.1 Plan view (cf. figure 3)

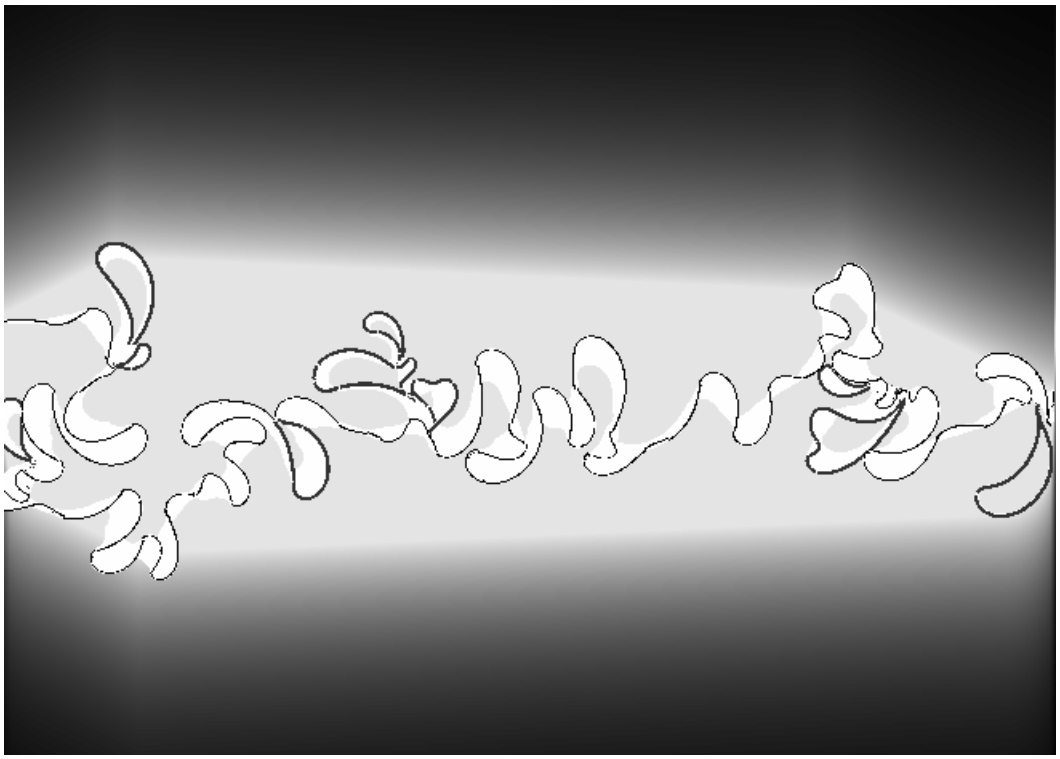

Figure 3: Plan view of a simulated floodplain. The white intensity codes the sand proportion. The thin black line across the floodplain is the channel centerline. The oxbow lakes are simulated by filling the abandoned loops with clay and are the wider black lines. Overbank deposits are simulated first by computing the channel centerline convex hull and filling it with a high proportion of silt and sand. Outside this rough meandering belt, sediment grain-size and thickness is decreasing exponentially with the distance to the convex hull. Floodplain length is about 15 km and floodplain width is about 10 km.

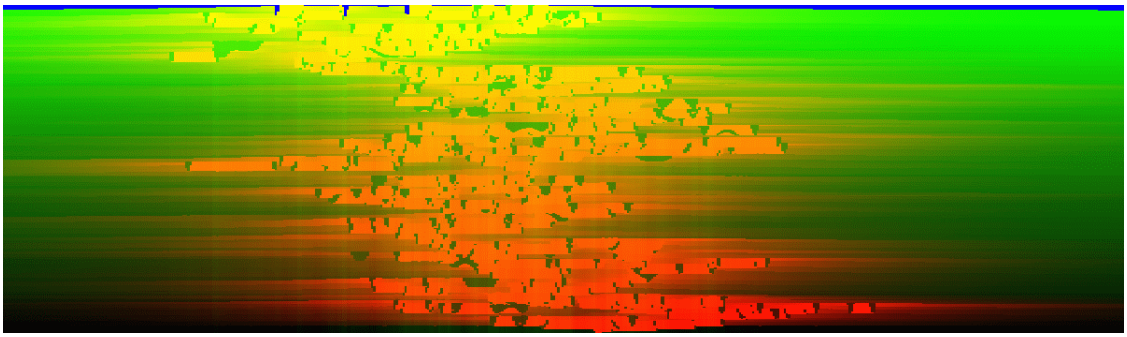

Figure 4: Vertical cross section across the simulated floodplain represented in figure 3. Sand bodies are coded in red for the older ones going through to yellow for the younger ones. Clays are coded in black green for the older ones going through to bright green for the younger ones. The successive migrations of the channel and distinct sand bodies are clearly identified. This cross section also illustrates the importance of simulating mud plugs (green *stains*) which can alter the connectivity between sand units. The cross section is about 10 km wide and 30 m thick.

3.2.2 Vertical cross-section (cf. figure 4)

3.2.3 Three dimensional view (cf. figure 5)

4 Stochastic aspects

Some stochastic aspects have already been observed in the influence of the initial conditions on the exact location of the meander loops. Herein, our final goal is to study how the simulations could be conditioned to respect given proportion curves. Indeed, geostatistical simulation respecting vertical proportion curves of facies have proved to efficiently reproduce the heterogeneity and distribution of deposits [Ravenne et al., 2000]. With these objectives in mind this last part focuses on the effect of the variations of a few parameters on the vertical proportion curves, at the scale of the floodplain and then more locally.

4.1 Floodplain scale

As many parameters can be studied (geometrical parameters of the channel, floodplain slope...), we will only focus on a few number controlling overbank deposition and thus floodplain accretion.

4.1.1 Varying parameters controlling overbank deposition

Varying the proportion of sand and silt deposited in the meandering belt and varying the parameters controlling the exponential decrease of thickness and grain-size, the average

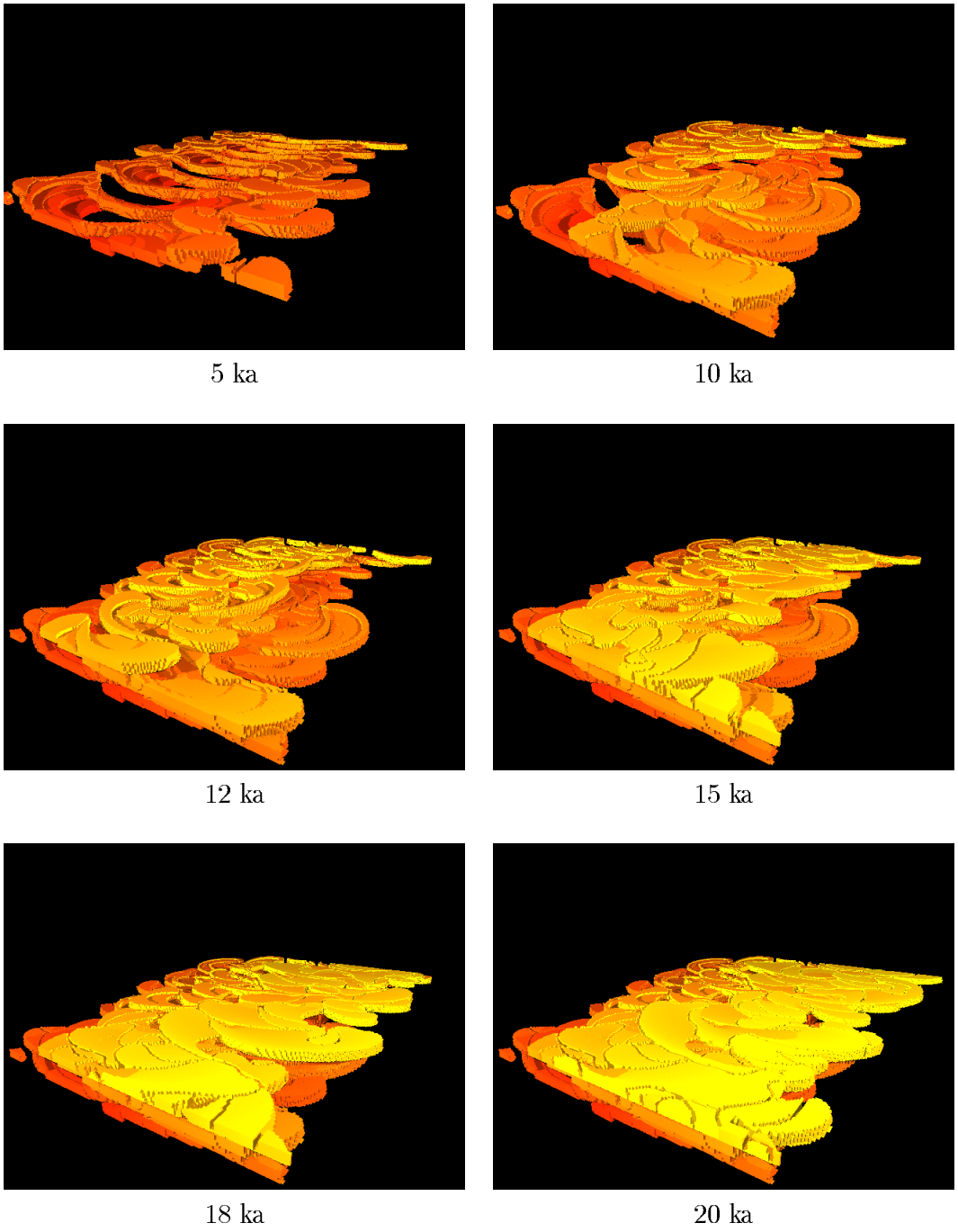

Figure 5: Successive sandy point-bar deposits over a 20 ka period. Sand bodies are coded in red for the older ones going through to yellow for the younger ones. These three dimensional views show how intricate and complex the meandering patterns can be at the scale of the oil reservoir. These views were obtained by removing silt and clays from a 3 km long, 2 km wide and 5 m high parallelepiped.

proportions of facies at floodplain scale can be changed. Such an example is given in figure 6.

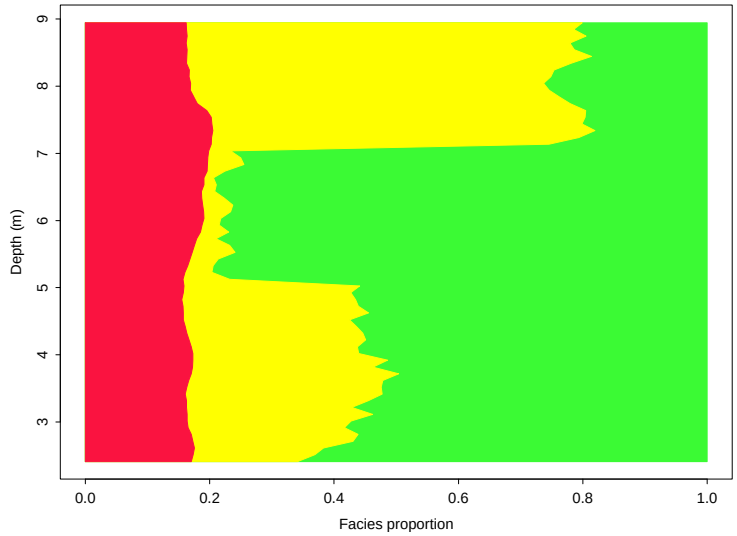

Figure 6: Vertical proportion curve of a floodplain simulated varying the parameters controlling the exponential decrease of deposits' grain-size outside the meandering belt. Sand facies is coded in red, silt facies is coded in yellow and clay facies is coded in green. Considering distinct parameters can control the respective proportions of silt and clays.

4.1.2 Varying the frequency and intensity of overbank floods

It is also of interest to consider the variability of overbank floods. Herein they have been simulated as Poisson point processes and their intensity was assumed to follow a normal law whose mean and variance were given. The floodplain formation was simulated over a period of 120 ka, and divided into three periods of 40 ka.

- During the first period of 40 ka a high frequency of overbank floods was imposed leading to quick floodplain vertical aggradation ;

- Then, in the second part the frequency of overbank floods was lowered. Consequently between two floods the channel has the time to migrate all across the floodplain forming large point-bar deposits. As a result this period with a few overbank floods corresponds to the deposition of a level with a high proportion of sand ;

- Finally, in the last 40 ka period frequent overbank floods were imposed again with a quick floodplain vertical aggradation.

If the vertical proportion curve is computed for the entire floodplain (cf. figure 7) it clearly stresses the existence of a level with a high proportion of sand that corresponds to the period of the low frequency of floods. So, varying the floods can be a way to condition the distribution of sand at the scale of the floodplain. Yet, to condition more precisely this distribution, the meandering belt location has to be constrained to determined areas.

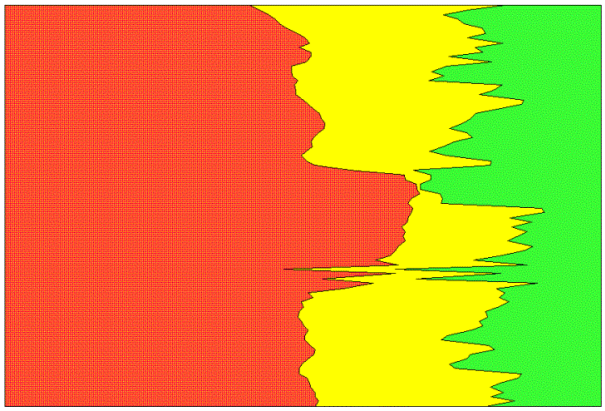

Figure 7: Vertical proportion curve of a floodplain simulated varying the frequency and intensity of overbank floods. Color coding and legend are the same as for figure 6, see text for comments.

4.2 Meander loop scale

4.2.1 Conditional erodibility maps

The erodibility coefficient E, introduced in the bank retreat equation 5, links soil nature and meander migration intensity. Thus we considered it as a regionalized variable representing a spatial heterogeneity. We carried out a conditional simulation for E this in order to study the influence of highly erodible areas to attract the channel and once attracted to confine the channel. The results obtained with such erodibility maps are shown on figure 8 It proved an effective way for conditioning the meandering belt location and consequently, the distribution of facies across the floodplain.

4.2.2 Gradually changing the erodibility maps

As the floodplain progressively aggrades with the successive overbank floods, the meandering belt slowly shifts too. Consequently to take into account this shifting and to constrain

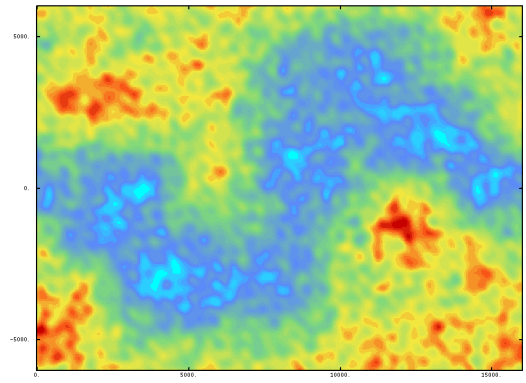

Conditional simulation for E

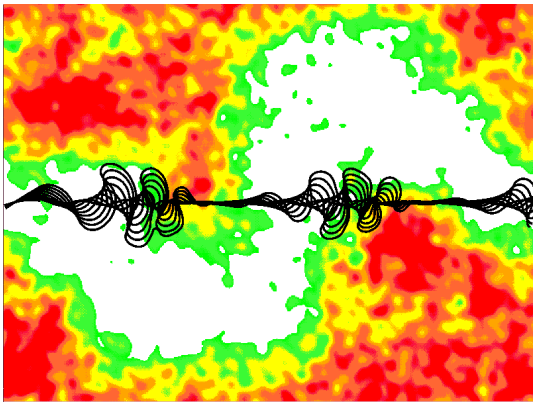

Channel location: 0 - 4 ka

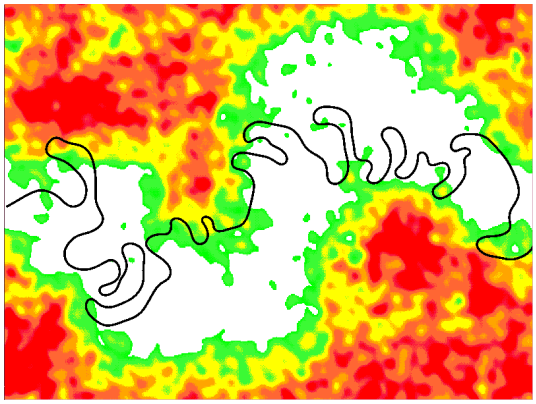

Channel location: 10 ka

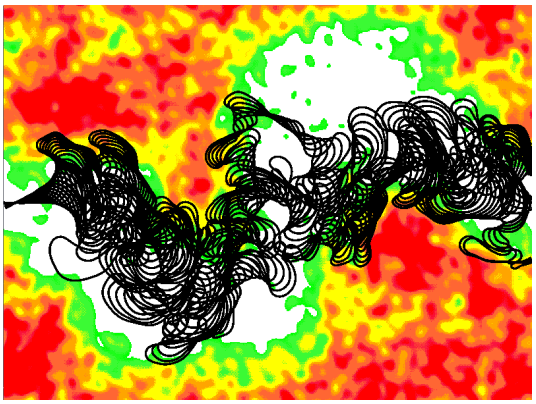

Channel location: 12 - 16 ka

Figure 8: Conditioning of the meandering belt by the use of conditional erodibility maps. The blue zone on the top left figure is the imposed area of high erodibility. As the channel evolves faster in this area, the cutoffs preferentially and successively occur there, what progressively attract the channel. Then, once attracted, the channel remains constrained to this artificial valley of high erodibility. The simulated floodplain is about 15 km long and about 10 km wide.

it the erodibility maps can be continuously changed using the gradual deformation algorithm of Hu ([Matheron, 1982], [Hu, 2000]).

This method was used to simulate the meandering belt shifting over a period of about 40 ka, gradually passing from one erodibility map to another. Then a square shaped area of the floodplain was divided into 81 smaller squares and for each of these sub-domains the vertical proportion curves were computed. The results are shown on figure 9. They clearly stress the temporal local evolution of facies: some areas pass from sand and silt to clay while other areas have the reverse evolution.

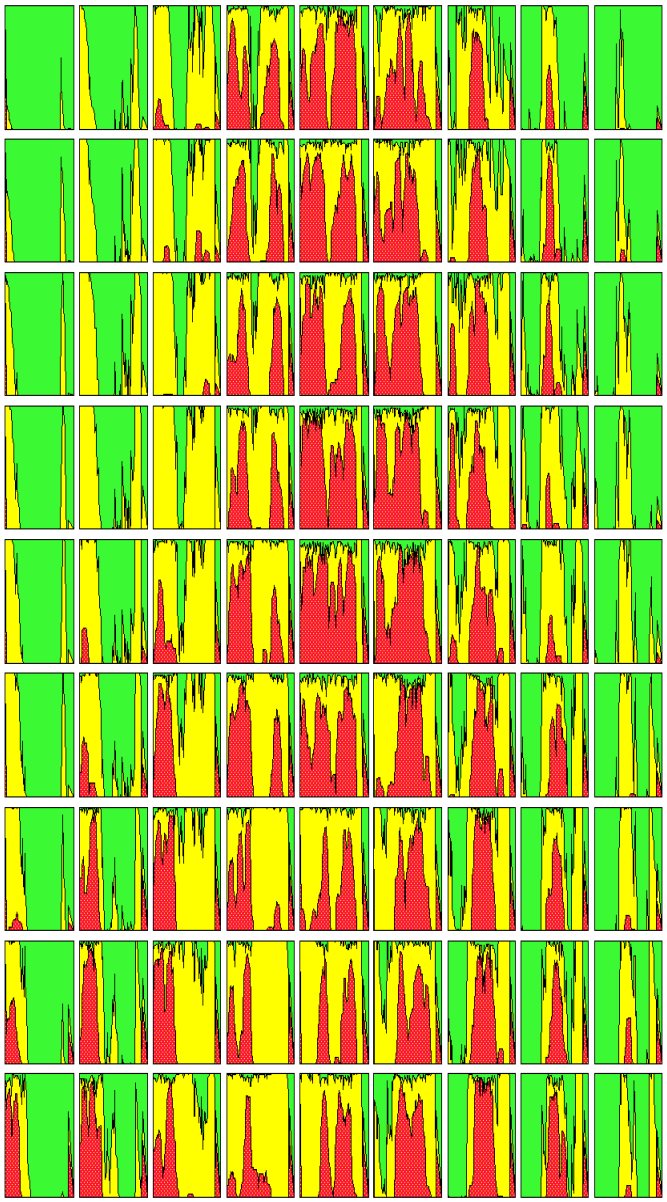

Figure 9: Distribution of facies across the floodplain when the shifting of the meandering belt is simulated using the gradual deformation algorithm. Each of the vertical proportion curves is computed for a 800 m x 800 m square area of the floodplain. All these areas are contiguous and they form a 7.2 km x 7.2 km larger domain. See text for comments.

5 Conclusions and perspectives

The present model remains very simplistic as it only takes account of vertical aggradation and does not deal with incision of valleys. It doesn't take account either of processes such as chute cutoffs, crevasse splays or avulsions which is particularly unrealistic in an aggradational context. Yet it provides quick and realistic representations of floodplain and channel deposits which enable the good localization and evaluation of sand bodies and mud plugs. Varying some parameters controlling the deposition the distribution of facies can be globally constrained at the scale of the floodplain. Then, additional use of different conditional erodibility maps provides an efficient way of confining the channel to successive areas and to refine this distribution of facies.

The next step of this work is to take into account avulsion processes and try to condition the model to given proportion curves. It would also be interesting to consider cycles not only of aggradation but also of incision to accurately reproduce the reality of geological cycles.

References

[Díaz-Molina et al., 1995] Díaz-Molina, M., Arribas, J., Gómez, J., and Tortosa, A. (1995). Geological modelling of a reservoir analogue: Cenozoic meander belts, loranca basin, spain. *Petroleum Geoscience*, 1(1):43–48.

[Howard, 1992] Howard, A. D. (1992). *Lowland Floodplain Rivers : Geomorphological Perspectives*, chapter Modelling channel migration and floodplain sedimentation in meandering streams, pages 1–37. John Wiley and Sons.

[Howard, 1996] Howard, A. D. (1996). *Floodplain Processes*, chapter Modelling channel evolution and floodplain morphology, pages 15–62. John Wiley and Sons.

[Hu, 2000] Hu, L. (2000). Gradual deformation of non-gaussian stochastic simulations. In *Geostats 2000 South Africa*.

[Ikeda et al., 1981] Ikeda, S., Parker, G., and Sawai, K. (1981). Bend theory of river meanders. part 1. linear development. *Journal of Fluid Mechanics*, 112:363–377.

[Johanesson and Parker, 1989] Johanesson, H. and Parker, G. (1989). *River Meandering*, chapter Linear theory of river meanders, pages 181–213. Water Resources Monograph. American Geophysical Union.

[Matheron, 1982] Matheron, G. (1982). La destructuration des hautes teneurs et le krigeage des indicatrices. Technical report, CGMM N-761, Centre de Géostatistique, Ecole des Mines de Paris.

[Ravenne et al., 2000] Ravenne, C., Galli, A., Doligez, B., Beucher, H., and Eschard, R. (2000). Quantification of faciès relationships via proportion curves. In *Proceedings of the 31st International Geological Congress*.

[Sun, 1998] Sun, T. (1998). *Computer simulations on meandering, braided rivers and fluvial fan-deltas*. PhD thesis, Department of Physics, University of Oslo.

[Sun et al., 1996] Sun, T., Meakin, P., Jossang, T., and Schwartz, K. (1996). A simulation model for meandering rivers. *Water resources research*, 32(9):2937–2954.

[Thorne et al., 1997] Thorne, C. R., Hey, R. D., and Newson, M. D., editors (1997). *Applied fluvial geomorphology for river engineering and management*, chapter Bank erosion and instability, pages 137–172. John Wiley & Sons.